Pressure Effect Determined with Use of the Nondispersive Infrared Gas Analyser

Eiji Niki and Tsutomu Yonezawa
Department of Industrial Chemistry, Faculty of Engineering, Tokyo University, Hongo, Tokyo 113

(Received June 16, 1972)

The pressure effect of nitrous oxide and nitric oxide due to nitrogen gas was investigated with use of a nondispersive infrared gas analyser. The results are in line with the theoretical curves derived from the Elsasser theory. The calculated expression is partly improved and the error of calculations is estimated in regard to carbon dioxide.

With a nondispersive infrared gas analyser, it is easily observed that the absorption increases with increasing pressure of nitrogen gas at constant pressure of infrared absorbing gases such as carbon dioxide or carbon monoxide. This effect is known as the pressure broadening. In a previous paper[1] the mean absorption was calculated on the Elsasser theory as a function of the partial pressure of absorber, the total pressure and the length of the sample cell. The result was proved to interpret fairly well the experimental results for carbon dioxide and carbon monoxide. In this paper, the influence of the Bessel function of order zero approximated by unit is evaluated in regard to carbon dioxide. Experiments were carried out on nitrous oxide and nitric oxide concerning the self broadening of the absorbing gas and the foreign gas broadening due to nitrogen gas in order to see whether the result of calculation can be applied to other infrared absorbing gases.

Apparatus

The apparatus consists of a nondispersive infrared gas analyser of the zero method positive filter type with a condenser microphone detector.[2] The windows consist of LiF. A schematic diagram is given in Fig. 1.

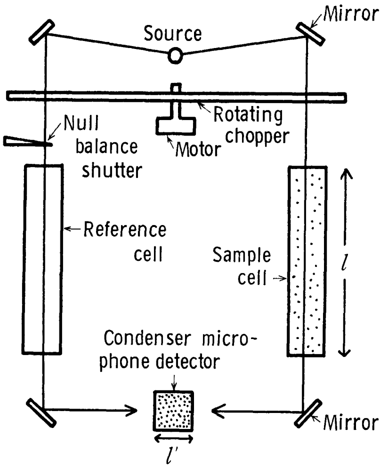

Fig. 1. The schematic diagram of the nondispersive infrared gas analyser. The temperature of the infrared source is about 600 °C. $l'=5$ cm.

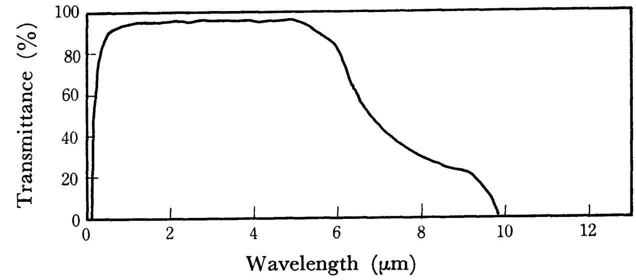

Fig. 2. The spectral transmission of LiF.

The sample gas is prepared in the mixing vessel and its pressure is measured by a mercury manometer. Figure 2 shows the spectral transmission of lithium fluoride.[3] Its absorption edge is about 1030 cm^{-1}.

Theoretical

For the sake of simplicity let us consider the expression

$$y=\frac{\int_0^\infty \{1-\exp(-\sum_{m=1}^{n} k_m l)\}\mathrm{d}\nu}{nd} \tag{1}$$

which gives the mean absorption of the band spectrum in the infrared region, where k_m is the absorption coefficient of each vibrational rotational line, m the number added to each line, n the total number of lines, d the line spacing and l the thickness of the layer. The absorption coefficient k_m, in general, can be expressed by means of the Lorentz curve

$$k_m=\frac{(\alpha_m/\pi)\delta}{(\nu-\nu_m)^2+\delta^2} \tag{2}$$

ν_m being the frequency at the center of the mth line. α_m is equivalent to $\int_0^\infty k_m \mathrm{d}\nu$ and assumed to be proportional to the partial pressure of absorber p_a,

$$\alpha_m=\alpha_{0m}p_a \tag{3}$$

α_{0m} being the proportional constant. δ is the damping constant and is known to be common to all the lines. From kinetic theory of the gas, δ is given by[4]

$$\delta=\frac{1}{4\pi}\sum_i N_i(D_{a,i})^2\left[2\pi kT\left(\frac{1}{m_a}+\frac{1}{m_i}\right)\right]^{1/2} \tag{4}$$

where N_i is the number of molecules of the ith type gas per unit volume, $D_{a,i}$ the sum of the optical col-

---

[1] T. Yonezawa and E. Niki, *Trans. Soc. Instr. Cont. eng.*, **7**, 236 (1970).

[2] D. W. Hill and T. Powell, "Non-Dispersive Infrared Gas Analyser," Plenum Press: New York (1968) p. 1.

[3] D. W. Hill and T. Powell, *ibid.*, p. 20.

[4] D. E. Burch, E. B. Singleton, and D. Williams, *Appl. Opt.*, **1**, 359 (1962).

lision diameters of the absorbing molecule and a molecule of the ith type, m_a the mass of the absorbing molecule and m_i the mass of the ith type of molecule. Replacing the number of molecules N_i by the corresponding partial pressure p_i in Eq. (4), we have

$$\delta = \frac{1}{4\pi}\left(\frac{2\pi}{kT}\right)^{1/2} \sum_i C_{a,i}p_i \tag{5}$$

where $C_{a,i}$ is a constant involving the masses and optical collision diameters of the absorbing and ith gas, respectively. If Eq. (5) is restricted to the binary mixtures, then

$$\delta = \frac{1}{4\pi}\left(\frac{2\pi}{kT}\right)^{1/2} (C_{a,a}p_a + C_{a,b}p_b) \tag{6}$$

where a refers to the absorbing molecule and b the foreign molecule. From Eq. (6) we get

$$\delta = \frac{1}{4\pi}\left(\frac{2\pi}{kT}\right)^{1/2} C_{a,a}\{p_a + (C_{a,b}/C_{a,a})p_b\}. \tag{7}$$

The expression in parentheses gives the effective pressure P_e of the gas mixture. If we denote coefficient $1/4\pi(2\pi/kT)^{1/2}C_{a,a}$ by a δ_0, then δ is given by

$$\delta = \delta_0 P_e. \tag{8}$$

For binary mixtures, we have $P_e = p_a + (1/B)p_b$ where $B = C_{a,a}/C_{a,b}$ which is called the self-broadening coefficient[5] of the absorbing gas which represents the ratio of the self-broadening ability of the absorbing gas to the broadening ability of the broadening gas. p_b is the partial pressure of the broadening gas.

If each of the n vibrational rotational lines is supposed to be completely isolated from the neighboring lines, Eq. (1) reduces to

$$y = \frac{\sum_{m=1}^{n} \int_u^v \{1-\exp(-k_m l)\}\mathrm{d}\nu}{nd} \tag{9}$$

u, v being $\nu_m - d/2$ and $\nu_m + d/2$. Introducing the following mean fractional transmission of mth line T_m defined by Elsasser[6]

$$T_m = \frac{1}{d}\int_u^v \exp\left\{-\frac{(\alpha_m/\pi)\delta}{(\nu-\nu_m)^2+\delta^2}\,l\right\}\mathrm{d}\nu, \tag{10}$$

Eq. (9) becomes

$$y = 1 - \langle T_m \rangle_{\mathrm{av}} \tag{11}$$

where $\langle\ \rangle_{\mathrm{av}}$ indicates the average of T_m over m, *viz.*, $\langle T_m\rangle_{\mathrm{av}} = 1/n \sum_{m=1}^{n} T_m$. T_m was evaluated by Elsasser in regard to the limits of small and large δ. If δ is small compared with the line spacing d, then

$$T_m = 1 - \phi\{(\pi\alpha_m\delta l)^{1/2}/d\} \tag{12}$$

where ϕ is probability integral. Here ϕ is supposed to be approximated by

$$\phi\{(\pi\alpha_m\delta l)^{1/2}/d\} = 2(\alpha_m\delta l)^{1/2}/d. \tag{13}$$

Thus we have

$$y = 2\langle(\alpha_m\delta l)^{1/2}/d\rangle_{\mathrm{av}}. \tag{14}$$

By means of Eqs. (3) and (8), the equation becomes

$$y = 2\left\langle\frac{\alpha_{0m}^{1/2}\delta_0^{1/2}}{d}\right\rangle_{\mathrm{av}} p_a^{1/2}P_e^{1/2}l^{1/2}. \tag{15}$$

If δ is large compared with the line spacing, then

$$T_m = \exp\{-(\alpha_m l/d)\tanh 2\beta\} \times J_0\{i(\alpha_m l/d)\tanh 2\beta/\cosh 2\beta\} \tag{16}$$

where $\beta \equiv \pi\delta/d$ and J_0 is the Bessel function of order zero and imaginary argument. By replacing $\tanh 2\beta$ with 2β and J_0 with the unit in Eq. (16), we get

$$T_m = \exp(-2\pi\alpha_m\delta l/d^2). \tag{17}$$

Substituting Eq. (17) into Eq. (11) and using Eqs. (3) and (8), we have

$$\begin{aligned} y &= 1 - \langle\exp\{-2\pi(\alpha_{0m}\delta_0/d^2)p_aP_el\}\rangle_{\mathrm{av}} \\ &= 1 - \langle\exp\{-2\pi(\alpha_{0m}\delta_0/d^2)P_ew\}\rangle_{\mathrm{av}} \end{aligned} \tag{18}$$

where the optical thickness $w = p_a l$ is used. Employing the cumulant expansion theorem in the calculation of $\langle\ \rangle_{\mathrm{av}}$ in Eq. (18), we get

$$\begin{aligned} y = 1 - \exp\Bigg\{ &-2\pi\left\langle\frac{\alpha_{0m}\delta_0}{d^2}\right\rangle_{\mathrm{av}} P_ew \\ &+ \frac{(2\pi)^2}{2\,!}\left(\left\langle\left(\frac{\alpha_{0m}\delta_0}{d^2}\right)^2\right\rangle_{\mathrm{av}} - \left\langle\frac{\alpha_{0m}\delta_0}{d^2}\right\rangle_{\mathrm{av}}^2\right)(P_ew)^2 \\ &- \frac{(2\pi)^3}{3\,!}\left(\left\langle\left(\frac{\alpha_{0m}\delta_0}{d^2}\right)^3\right\rangle_{\mathrm{av}} - 3\left\langle\left(\frac{\alpha_{0m}\delta_0}{d^2}\right)^2\right\rangle_{\mathrm{av}}\left\langle\frac{\alpha_{0m}\delta_0}{d^2}\right\rangle_{\mathrm{av}} \right. \\ &\qquad \left. + 2\left\langle\frac{\alpha_{0m}\delta_0}{d^2}\right\rangle_{\mathrm{av}}^3\right)(P_ew)^3 \\ &+ \cdots\cdots\Bigg\}. \end{aligned} \tag{19}$$

Here $\alpha_{0m}\delta_0/d^2$ can be approximately evaluated if the minimum transmittance T_m^{dis} is observed correctly. The observable minimum transmittance T_m^{dis} is given by

$$T_m^{\mathrm{dis}} = \int_0^\infty \exp\left[-\frac{(\alpha_m/\pi)\delta l}{(\nu-\nu_m)^2+\delta^2}\right] f(|\nu-\nu_m|, a)\mathrm{d}\nu \Big/ \int_0^\infty f(|\nu-\nu_m|, a)\mathrm{d}\nu \tag{20}$$

where $f(|\nu-\nu_m|, a)$ is the slit function, a being the slit width of apparatus. When the triangular form is used for the slit function, we have approximately[7]

$$T_m^{\mathrm{dis}} = 1 - 2(\alpha_m\delta l)^{1/2}/a + \cdots\cdots. \tag{21}$$

Thus

$$E_m = -\ln T_m^{\mathrm{dis}} = 2(\alpha_m\delta l)^{1/2}/a \tag{22}$$

for the maximum extinction E_m. If k_{0m} is defined by the relation

$$k_{0m} = E_m^2 \Big/ \left\{4\cdot\left(\frac{d}{a}\right)^2 p_a^2 l\right\}, \tag{23}$$

then the following relation is obtained by substituting Eqs. (22), (3) and (8) into Eq. (23)

$$\alpha_{0m}\delta_0/d^2 = k_{0m} \tag{24}$$

provided that P_e of Eq. (3) is put equal to p_a. When the Gaussian form is used for the slit function, for example, the maximum extinction is

$$E_m = 1.879(\alpha_m\delta l)^{1/2}/a. \tag{25}$$

Thus if we assume that when the true slit function, not known beforehand, is used, the maximum extinction

---

[5] D. E. Burch, E. B. Singleton, and D. Williams, *Appl. Opt.* **1**, (1962).

[6] W. M. Elsasser, *Phys. Rev.*, **54**, 126 (1939).

[7] J. R. Nielsen, V. Thorton, and, E. B. Dale, *Rev. Mod. Phys.*, **16**, 308 (1944).

is given by

$$E_m = t(\alpha_m \delta l)^{1/2}/a\,, \tag{26}$$

then

$$\alpha_{0m}\delta_0/d^2 = (2/t)^2 \cdot k_{0m} \tag{27}$$

where t is the constant which is determined if the true slit function is known.

Quantity x, which is measured as the absorption ratio due to the sample gas at the nondispersive infrared gas analyser, is obtained from the following relation

$$(1-x)\int_0^\infty I_\nu \{1-\exp(-\sum_{m=1}^{n} k'_m l')\}\mathrm{d}\nu$$
$$= \int_0^\infty I_\nu \exp(-\sum_{m=1}^{n} k_m l)\{1-\exp(-\sum_{m=1}^{n} k'_m l')\}\mathrm{d}\nu \tag{28}$$

where I_ν is the energy distribution of the infrared source, k_m and l the absorption coefficient and the cell length of the sample, and k'_m and l' of the condenser microphone detector. k'_m is given by

$$k'_m = \frac{(\alpha'_m/\pi)\delta'}{(\nu-\nu_m)^2+\delta'^2}\,.$$

The same gas as in the absorber is sealed up within the detector in atmospheric pressure. Equation (28) shows that the left-hand gives the energy absorbed in the detector of the infrared ray screened by the null balance shutter and the right-hand the energy absorbed in the detector of the infrared ray passing through the sample cell. Thus we have from Eq. (28)

$$x = \frac{\int_0^\infty I_\nu \{1-\exp(-\sum_{m=1}^{n} k_m l)\}\{1-\exp(-\sum_{m=1}^{n} k'_m l')\}\mathrm{d}\nu}{\int_0^\infty I_\nu \{1-\exp(-\sum_{m=1}^{n} k'_m l')\}\mathrm{d}\nu}\,. \tag{29}$$

For the calculation of Eq. (29) the following two assumptions are made; (i) I_ν=const. over the absorption region of the sample gas, and (ii) the shape of $\{1-\exp(-\sum_{m=1}^{n} k_m{}'l')\}$ is approximated by the n equivalent rectangles with unit height and the width of d' which varies with l' or the conditions under which the absorbing gas is sealed within the detector. Thus, x is given by

$$x = \sum_{m=1}^{n}\int_{u'}^{v'} \{1-\exp(-k_m l)\}\mathrm{d}\nu/nd'. \tag{30}$$

It is assumed herewith that each of the n vibrational rotational lines are completely isolated from the neighboring lines. u' and v' are $\nu_m - d'/2$ and $\nu_m + d'/2$. Eq. (30) corresponds to replacing d in Eq. (9) with d'. Thus from Eqs. (15) and (19), the expressions for x at low and high pressure are obtained by replacing d in each eq. with d'. From Eq. (15) we get

$$x = 2\left\langle\frac{\alpha_{0m}^{1/2}\delta_0^{1/2}}{d'}\right\rangle_{\mathrm{av}} p_{\mathrm{a}}{}^{1/2}P_{\mathrm{e}}{}^{1/2}l^{1/2} \tag{31}$$

and from Eq. (19)

$$x = 1 - \exp\Bigg\{-2\pi\left\langle\frac{\alpha_{0m}\delta_0}{d'^2}\right\rangle_{\mathrm{av}} P_{\mathrm{e}}w$$
$$+\frac{(2\pi)^2}{2\,!}\left(\left\langle\left(\frac{\alpha_{0m}\delta_0}{d'^2}\right)^2\right\rangle - \left\langle\frac{\alpha_{0m}\delta_0}{d'^2}\right\rangle_{\mathrm{av}}^2\right)(P_{\mathrm{e}}w)^2$$

$$-\frac{(2\pi)^3}{3\,!}\left(\left\langle\left(\frac{\alpha_{0m}\delta_0}{d'^2}\right)^3\right\rangle_{\mathrm{av}} - 3\left\langle\left(\frac{\alpha_{0m}\delta_0}{d'^2}\right)^2\right\rangle_{\mathrm{av}}\left\langle\frac{\alpha_{0m}\delta_0}{d'^2}\right\rangle_{\mathrm{av}}\right.$$
$$\left. + 2\left\langle\frac{\alpha_{0m}\delta_0}{d'^2}\right\rangle_{\mathrm{av}}^3\right)(P_{\mathrm{e}}w)^3$$
$$+ \cdots\cdots\cdots\Bigg\}\,. \tag{32}$$

From Eq. (27) we get

$$\alpha_{0m}\delta_0/d'^2 = (2/t)^2 \cdot (d/d')^2 \cdot k_{0m} \tag{33}$$

Replacing $(2/t)\cdot(d/d')$ with $1/D$, we get

$$\alpha_{0m}\delta_0/d'^2 = k_{0m}/D^2. \tag{34}$$

Rewriting Eqs. (31) and (32) by means of this relation, we get

$$x = 2(\langle k_{0m}^{1/2}\rangle_{\mathrm{av}}/D)p_{\mathrm{a}}{}^{1/2}P_{\mathrm{e}}{}^{1/2}l^{1/2} \tag{35}$$

and

$$x = 1 - \exp\Bigg\{-(2\pi/D^2)\,\langle k_{0m}\rangle_{\mathrm{av}}\cdot P_{\mathrm{e}}w$$
$$+\frac{(2\pi/D^2)^2}{2\,!}\,(\langle k_{0m}^2\rangle_{\mathrm{av}} - \langle k_{0m}\rangle_{\mathrm{av}}^2)\cdot(P_{\mathrm{e}}w)^2$$
$$-\frac{(2\pi/D^2)^3}{3\,!}\,(\langle k_{0m}^3\rangle_{\mathrm{av}} - 3\langle k_{0m}^2\rangle_{\mathrm{av}}\cdot\langle k_{0m}\rangle_{\mathrm{av}}$$
$$+ 2\,\langle k_{0m}\rangle_{\mathrm{av}}^3)\cdot(P_{\mathrm{e}}w)^3$$
$$+ \cdots\cdots\cdots\Bigg\}\,. \tag{36}$$

From Eq. (36), we get

$$\ln\frac{1}{1-x} = \sum_{n=1}^{\infty}(-1)^{n-1}\kappa_n(P_{\mathrm{e}}w)^n \tag{37}$$

where

$$\kappa_n = (2\pi/D^2)^n\lambda_n/n\,!$$

λ_n being the cumulant coefficient.

If there exists another weak band, for example a combination band, r, the ratio of the intensity of the infrared source of the fundamental region to that of the combination, should be introduced. Thus, assuming that the shape of the absorption line of the detector is approximated by the $n+n'$ equivalent rectangles with unit height and the average width d'' over both band, we obtain the following relation from Eq. (29):

$$x = \frac{\sum_{m=1}^{n}\int_{u'}^{v'} I_{\mathrm{f}}\{1-\exp(-k_m l)\}\mathrm{d}\nu + \sum_{m'=1}^{n'}\int_{u''}^{v''} I_{\mathrm{c}}\{1-\exp(-k_{m'}l)\}d\nu}{(I_{\mathrm{f}}\cdot n + I_{\mathrm{c}}\cdot n')d''}$$
$$= \frac{\sum_{m=1}^{n}\int_{u'}^{v'}\{1-\exp(-k_m l)\}\mathrm{d}\nu + r\sum_{m'=1}^{n'}\int_{u''}^{v''}\{1-\exp(-k_{m'}l)\}\mathrm{d}\nu}{(n+rn')d''} \tag{38}$$

where m' is the number added to the lines in the combination band, u' and v' represent $\nu_m - d''/2$ and $\nu_m + d''/2$, u'' and v'' are $\nu_{m'} - d''/2$ and $\nu_{m'} + d''/2$, the constant quantities I_{f} and I_{c} are the intensities of the infrared source over the fundamental region and the combination, r is the ratio $I_{\mathrm{c}}/I_{\mathrm{f}}$, and n' is the total number of lines of the combination band. If we put $n'=n$ in Eq. (38), then

$$x=\frac{\sum\limits_{m=1}^{n}\int_{u'}^{v'}\{1-\exp(-k_m l)\}\mathrm{d}\nu+r\sum\limits_{m'=1}^{n}\int_{u''}^{v''}\{1-\exp(-k_m\, l)\}\mathrm{d}\nu}{(1+r)nd''}. \tag{39}$$

From this relation we get the following expression of x for low pressures

$$x = 2\left(\frac{\langle k_{0m}^{1/2}\rangle_{\mathrm{av}}+r\langle k_{0m'}^{1/2}\rangle_{\mathrm{av}}}{(1+r)D}\right)p_{\mathrm{a}}{}^{1/2}P_{\mathrm{e}}{}^{1/2}l^{1/2} \tag{40}$$

and that of x for high pressures

$$\begin{aligned}x=1-\exp\Bigg[&-(2\pi/D^2)\cdot\left(\frac{\langle k_{0m}\rangle_{\mathrm{av}}+r\langle k_{0m'}\rangle_{\mathrm{av}}}{1+r}\right)P_{\mathrm{e}}w\\&+\frac{(2\pi/D^2)^2}{2\,!}\left(\frac{\langle k_{0m}^2\rangle_{\mathrm{av}}+r\langle k_{0m'}^2\rangle_{\mathrm{av}}}{1+r}-\frac{\langle k_{0m}\rangle_{\mathrm{av}}^2+r\langle k_{0m'}\rangle_{\mathrm{av}}^2}{1+r}\right)\cdot\\&(P_{\mathrm{e}}w)^2-\frac{(2\pi/D^2)^3}{3\,!}\Bigg\{\frac{\langle k_{0m}^3\rangle_{\mathrm{av}}+r\langle k_{0m'}^3\rangle_{\mathrm{av}}}{1+r}\\&\quad-3\left(\frac{\langle k_{0m}^2\rangle_{\mathrm{av}}+r\langle k_{0m'}^2\rangle_{\mathrm{av}}}{1+r}\right)\cdot\left(\frac{\langle k_{0m}\rangle_{\mathrm{av}}+r\langle k_{0m'}\rangle_{\mathrm{a}}}{1+r}\right)\\&\quad+2\left(\frac{\langle k_{0m}\rangle_{\mathrm{av}}^3+r\langle k_{0m'}\rangle_{\mathrm{av}}^3}{1+r}\right)\Bigg\}\cdot(P_{\mathrm{e}}w)^3\\&+\cdots\cdots\cdots\Bigg]\end{aligned} \tag{41}$$

where $1/D=(2/t)(d/d'')$.

In the case of CO_2 the following result is obtained by assuming that I_ν is expressed by Planck's law for temperature radiation and the temperature of the infrared source is 900 K,

$$r = 0.524 \tag{42}$$

since the combination band is observed in 3700 cm^{-1} region. The numerical values for CO_2 are as follows.

$$\begin{aligned}\langle k_{0m}^{1/2}\rangle_{\mathrm{av}} &= 5.85\times10^{-3}\ \mathrm{cm}^{-1/2}\cdot\mathrm{cmHg}^{-1}\\ \langle k_{0m'}^{1/2}\rangle_{\mathrm{av}} &= 1.05\times10^{-3}\ \mathrm{cm}^{-1/2}\cdot\mathrm{cmHg}^{-1}\\ \frac{\langle k_{0m}^{1/2}\rangle_{\mathrm{av}}+r\langle k_{0m'}^{1/2}\rangle_{\mathrm{av}}}{1+r} &= 4.19\times10^{-3}\ \mathrm{cm}^{-1/2}\cdot\mathrm{cmHg}^{-1}\\ \frac{\langle k_{0m}\rangle_{\mathrm{av}}+r\langle k_{0m}\ \rangle_{\mathrm{av}}}{1+r} &= 3.77\times10^{-5}\ \mathrm{cm}^{-1}\cdot\mathrm{cmHg}^{-2}\\ \frac{\langle k_{0m}^2\rangle_{\mathrm{av}}+r\langle k_{0m'}^2\rangle_{\mathrm{av}}}{1+r} &= 4.48\times10^{-9}\ \mathrm{cm}^{-2}\cdot\mathrm{cmHg}^{-4}\\ \frac{\langle k_{0m}^3\rangle_{\mathrm{av}}+r\langle k_{0m'}^3\rangle_{\mathrm{av}}}{1+r} &= 6.50\times10^{-12}\ \mathrm{cm}^{-3}\cdot\mathrm{cmHg}^{-6}\end{aligned} \tag{43}$$

where 1.59 cm^{-1} is used as the values of the line spacing d.

Experimental

NO System. Figure 3 shows the relations between x and p_a of pure NO at low pressures. ○, △, □ represent the values corresponding to various cell lengths. As expected from Eq. (35), a linear relation is obtained between x and p_a in the case of pure NO where P_e can be put equal to p_a:

$$x = 2(\langle k_{0m}^{1/2}\rangle_{\mathrm{av}}/D)p_{\mathrm{a}}l^{1/2}. \tag{44}$$

The relations between x/p_a and $l^{1/2}$ are plotted by means of the relation in Fig. 3 (Fig. 4). From Eq. (44) we see that x/p^a is proportional to $l^{1/2}$. From the slope of this line, the proportionality constant $\langle k_{0m}^{1/2}\rangle_{\mathrm{av}}/D$ is found to be 3.00×10^{-3} $\mathrm{cm}^{-1/2}\cdot\mathrm{cmHg}^{-1}$. k_{0m} can be evaluated by the analysis of the infrared spectrum whose lines are adequately separated. The values of D is the factor that corrects the deviation between $\langle k_{0m}^{1/2}\rangle_{\mathrm{av}}$ and the value obtained above. The results for the binary mixture $NO+N_2$ are shown in Fig. 5, where the total pressure is kept constant. Broken lines represent the theoretical curves derived from Eq. (35). The self-broadening coefficient B is expreimentally given as 1.47. $\ln 1/(1-x)$ is plotted against the optical thickness w at the total pressure of 70 cmHg (Fig. 6). The solid line may be approximated by Eq. (35).

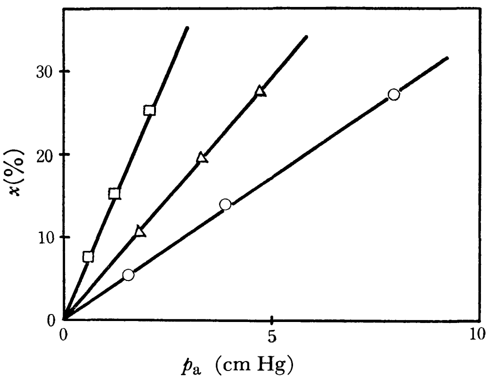

Fig. 3. Pure NO. cell length: 5 cm ○, 10 cm △ and 30 cm □.

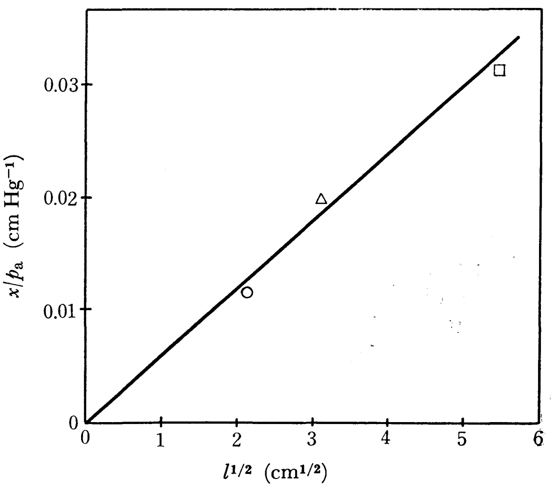

Fig. 4. Pure NO. the slope of the line$=6.00\times10^{-1/2}$ $\mathrm{cm}^{-1/2}\cdot\mathrm{cmHg}^{-1}$.

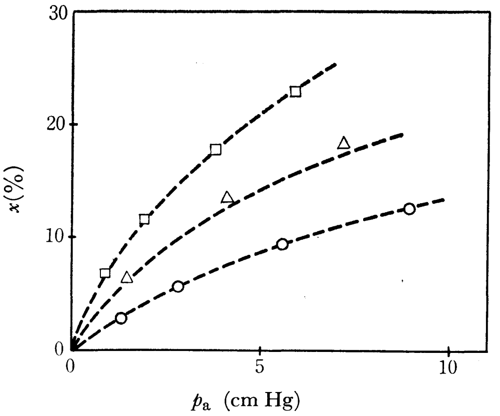

Fig. 5. $NO+N_2$ at the total pressure 10 cmHg.

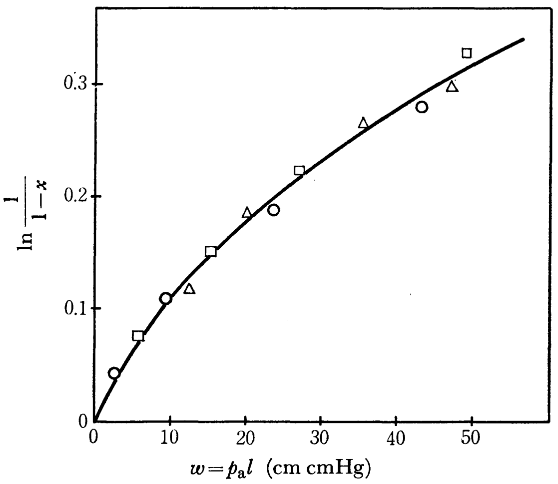

Fig. 6. NO+N_2 at the total pressure 70 cmHg.

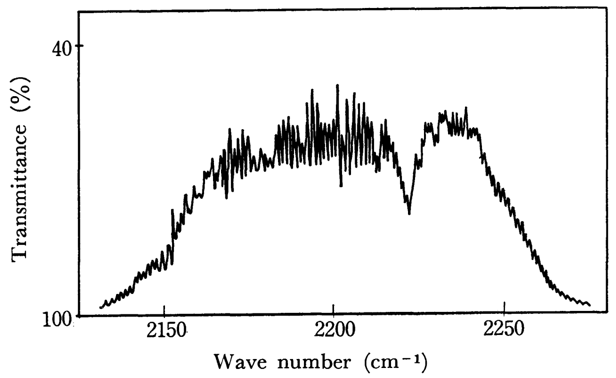

Fig. 7(a). Spectrum of N_2O around 2200 cm^{-1} measured on a DS-701G infrared spectrophotometer. slit width = 0.10 mm, cell length = 10.3 cm, concentration = 2.00 cmHg.

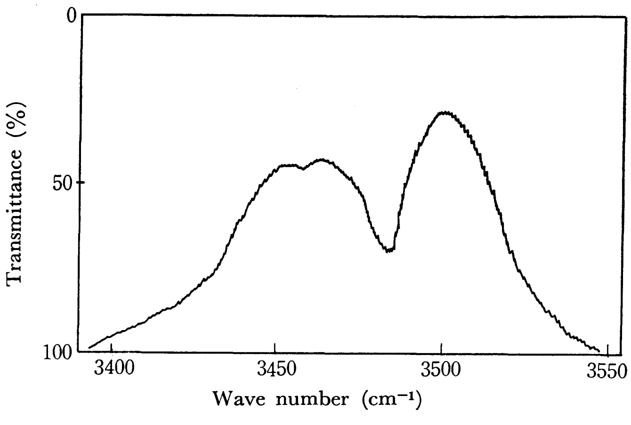

Fig. 7(b). Spectrum of N_2O around 3400 cm^{-1} measured on a DS-701G infrared spectrophotometer. slit width = 0.15 mm, cell length = 10.3 cm, concentration = 11.10 cmHg.

N_2O System. The infrared absorption spectra of N_2O are given in Fig. 7(a) and (b). The vibrational rotational lines around 2200 cm^{-1} region are imperfectly separated and those around 3400 cm^{-1} are no longer separated. When the separation of the lines is not enough, the analytical values of k_{0m} do not represent the values characteristic of the individual lines, because of the influence of the wings of the neighboring lines. Since the assumption that each line is separated is not valid, Eqs. (40) and (41) are not applied to N_2O. However, it is proved that these equations can

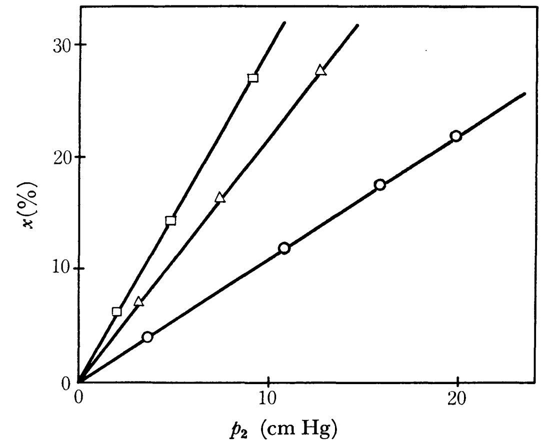

Fig. 8(a). Pure N_2O

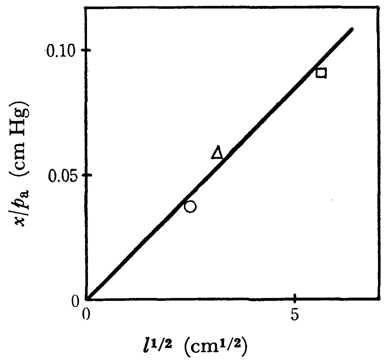

Fig. 8(b). Pure N_2O

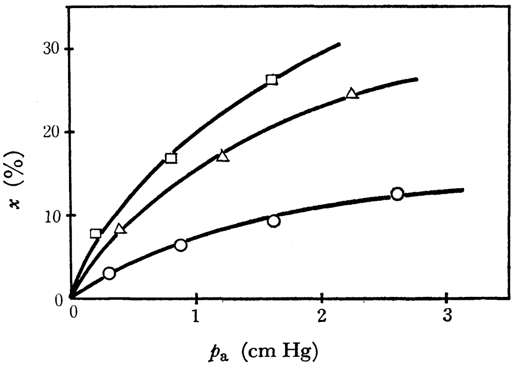

Fig. 8(c). N_2O+N_2 at the total pressure 5 cmHg.

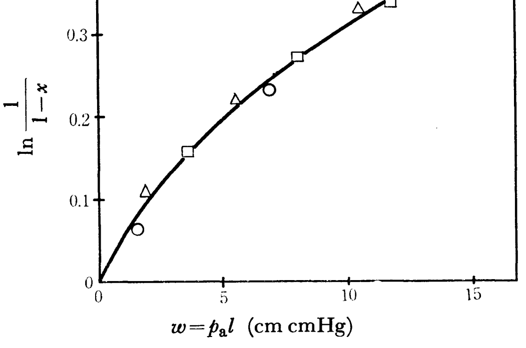

Fig. 8(d). N_2O+N_2 at the total pressure 70 cmHg.

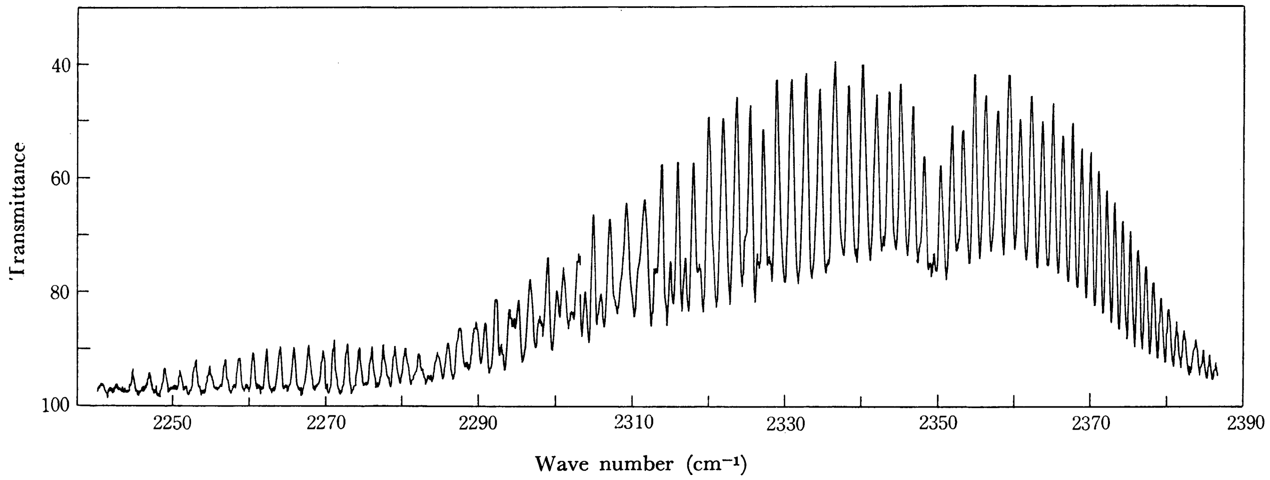

Fig. 9(a). Spectrum of CO_2 around 2350 cm^{-1} region due to the ν_3 fundamental. slit width = 0.20 mm, cell length = 10.3 cm, concentration = 2.00 cmHg. The infrared spectrophotometer is DS-403G.

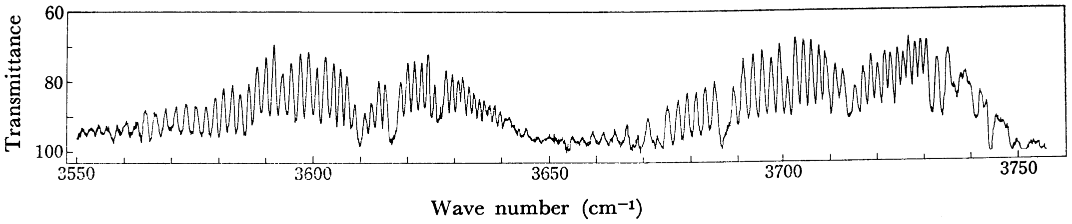

Fig. 9(b). Spectrum of CO_2 around the 2.7 μ region by the $\nu_1+\nu_3$ combination band at 3716 cm^{-1} and the $\nu_3+2\nu_2$ band at 3609 cm^{-1}. slit width = 0.10 mm, cell length = 10.3 cm, concentration = 9.60 cmHg. DS-403G.

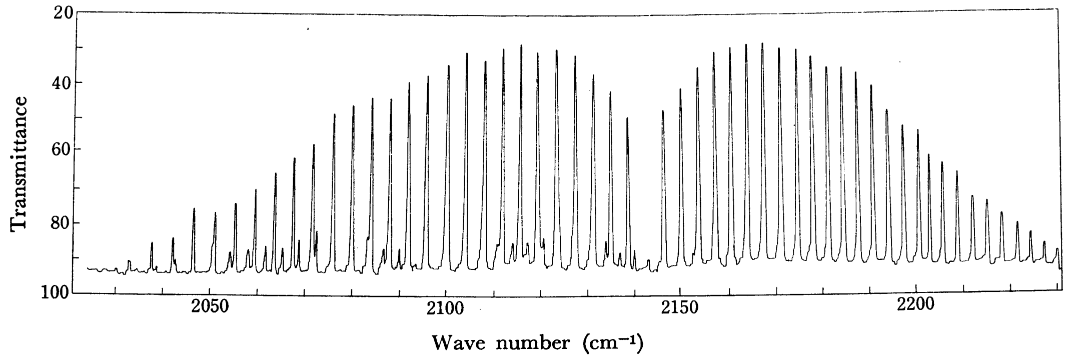

Fig. 9(c). Spectrum of CO around 2150 cm^{-1} measured on a DS-403G. slit width = 0.15 mm, cell length = 10.3 cm, concentration = 12.5 cmHg. DS-403G.

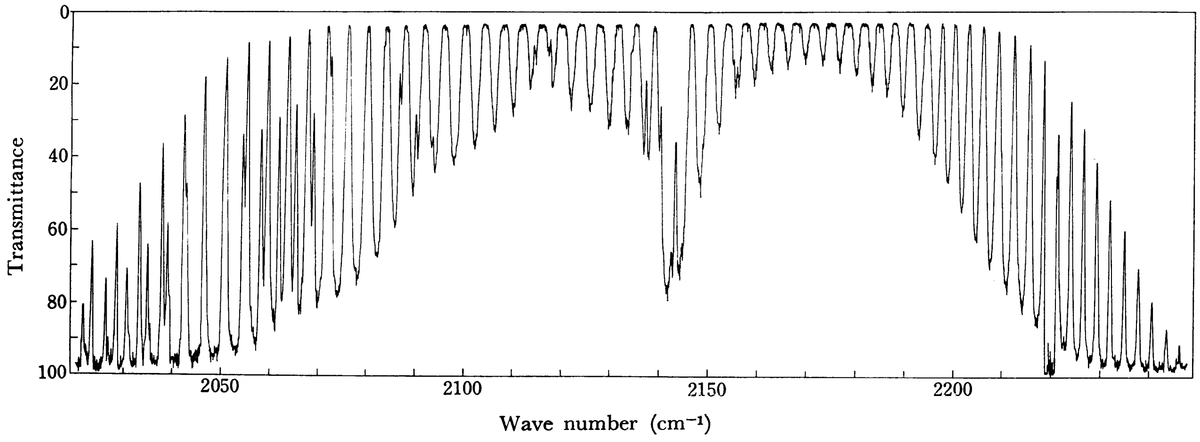

Fig. 9(d). Spectrum of CO around 2150 cm^{-1}. slit width = 0.15 mm, cell length = 10.3 cm, concentration = 1 atm. DS-403G.

be utilized for the quantitative interpretation of in the clination of the experimental curves of N_2O (Fig. 8).

Discussion

Degree of Separation of Absorption lines. The degree of separation of the absorption lines is determined from the line spacing and the collision width. The line spacing is inversely proportional to the moment of inertia which is geater for CO_2 than for CO. The collision width 2δ is given by Eq. (4). Putting $i=a$ in Eq. (4), δ is found to be proportional to $(D_{a,a})^2$-$(kT/m_a)^{1/2}N_a$. With the numerical data[8] $D_{a,a}/D_{a,i}=1.29$ where $a=CO_2$ and $i=CO$, we obtain

$$(D_{i,i}/D_{a,a})^2 = 0.30\,.$$

Since $(m_a/m_i)^{1/2}=1.24$, we get $\delta_i/\delta_a=0.37$. Thus the degree of separation is better for CO than for CO_2 (Fig. 9 (a)~(d)). The degree of separation influences the degree of accuracy of k_{0m}.

Influence of the Bessel Function of Order Zero. Considering the influence of the Bessel function of order zero, we have from Eq. (16):

$$\langle T_m\rangle_{av} = \langle \exp\{-(\alpha_m l/d')\tanh 2\beta'\} \times J_0\{i(\alpha_m l/d')\tanh 2\beta'/\cosh 2\beta'\}\rangle_{av} \tag{45}$$

where the line spacing d of Eq. (16) is replaced by the distance d', $\beta'=\pi\delta/d'$. Using the modified Bessel function of order zero, Eq. (45) is written as

$$\langle T_m\rangle_{av} = \langle \exp(-a_m)I_0(a_m/\cosh 2\beta')\rangle_{av} \tag{46}$$

where I_0 is the modified Bessel function of order zero, and

$$\begin{aligned} a_m &= (\alpha_m l/d')\tanh 2\beta' = (\alpha_m l/d')\cdot 2\beta'\varepsilon \\ &= 2\pi\varepsilon(\alpha_m \delta l/d'^2) = 2\pi\varepsilon(\alpha_{0m}\delta_0/d'^2)p_a P_e l \\ &= 2\pi\varepsilon(k_{0m}/D^2)P_e w\,, \end{aligned} \tag{47}$$

ε being $\varepsilon=(\tanh 2\beta')/2\beta'$, $I_0(a_m/\cosh 2\beta')$ is given by

$$I_0(a_m/\cosh 2\beta') = \sum_{n=0}^{\infty}\frac{1}{(n\,!)^2}\left(\frac{1}{2\cosh 2\beta'}\right)^{2n} a_m{}^{2n} \tag{48}$$

and hence

$$\begin{aligned}\langle T_m\rangle_{av} &= \left\langle \sum_{n=0}^{\infty}\frac{1}{(n\,!)^2}\cdot\frac{1}{(2\cosh 2\beta')^{2n}}\cdot a_m{}^{2n}\exp(-a_m)\right\rangle_{av} \\ &= \sum_{n=0}^{\infty}\frac{1}{(n\,!)^2}\cdot\frac{1}{(2\cosh 2\beta')^{2n}}\cdot\langle a_m{}^{2n}\exp(-a_m)\rangle_{av}\,. \end{aligned} \tag{49}$$

If $f(a_m, \xi)$ is defined by

$$f(a_m,\xi) \equiv \exp(-a_m\xi), \tag{50}$$

then $a_m{}^{2n}\exp(-a_m)$ is given by

$$a_m{}^{2n}\exp(-a_m) = \frac{d^{2n}}{d\xi^{2n}}f(a_m,\xi)\bigg|_{\xi=1} \tag{51}$$

and we obtain

$$\langle a_m{}^{2n}\exp(-a_m)\rangle_{av} = \frac{d^{2n}}{d\xi^{2n}}\langle f(a_m,\xi)\rangle_{av}\bigg|_{\xi=1}\,. \tag{52}$$

Consequently $\langle T_m\rangle_{av}$ becomes

$$\langle T_m\rangle_{av} = \sum_{n=0}^{\infty}\frac{1}{(n\,!)^2}\cdot\frac{1}{(2\cosh 2\beta')^{2n}}\cdot\frac{d^{2n}}{d\xi^{2n}}\langle f(a_m,\xi)\rangle_{av}\bigg|_{\xi=1}\,. \tag{53}$$

By use of the cumulant expansion theorem in $\langle f(a_m, \xi)\rangle_{av}$, we obtain

$$\langle f(a_m,\xi)\rangle_{av} = \exp\{h(\xi)\} \tag{54}$$

where

$$h(\xi) = -\langle a_m\rangle_c\xi + \frac{1}{2\,!}\langle a_m{}^2\rangle_c\xi^2 - \frac{1}{3\,!}\langle a_m{}^3\rangle_c\xi^3\,. \tag{55}$$

The higher terms than the third are ignored, $\langle a_m{}^n\rangle_c$ being the cumulant average of a_m of nth order. The derivatives of $\exp\{h(\xi)\}$ with respect to ξ are as follows.

$$\frac{d}{d\xi}\langle f(a_m,\xi)\rangle_{av} = h'(\xi)\exp\{h(\xi)\} \tag{56}$$

$$\frac{d^2}{d\xi^2}\langle f(a_m,\xi)\rangle_{av} = [h''(\xi)+\{h'(\xi)\}^2]\exp\{h(\xi)\} \tag{57}$$

$$\begin{aligned}\frac{d^3}{d\xi^3}\langle f(a_m,\xi)\rangle_{av} &= [h'''(\xi)+3h''(\xi)\cdot h'(\xi) \\ &\quad + \{h'(\xi)\}^3]\exp\{h(\xi)\}\end{aligned} \tag{58}$$

$$\begin{aligned}\frac{d^4}{d\xi^4}\langle f(a_m,\xi)\rangle_{av} &= [h''''(\xi)+4h'''(\xi)\cdot h'(\xi)+3\{h''(\xi)\}^2 \\ &\quad + 6\{h'(\xi)\}^2\cdot h''(\xi)+\{h'(\xi)\}^4]\exp\{h(\xi)\}\,.\end{aligned} \tag{59}$$

By substituting Eqs. (57) and (59) into Eq. (53), the following expression is obtained

$$\begin{aligned}\langle T_m\rangle_{av} = \Bigg[1 &+ \frac{1}{(2\cosh 2\beta')^2}\cdot\{(\langle a_m{}^2\rangle_c - \langle a_m{}^3\rangle_c) \\ &+ (\langle a_m\rangle_c - \langle a_m{}^2\rangle_c + \langle a_m{}^3\rangle_c/2)^2\} \\ &+ \frac{1}{4}\cdot\frac{1}{(2\cosh 2\beta')^4}\cdot\{4\langle a_m{}^3\rangle_c\cdot(\langle a_m\rangle_c - \langle a_m{}^2\rangle_c \\ &+ \langle a_m{}^3\rangle_c/2) + 3(\langle a_m{}^2\rangle_c - \langle a_m{}^3\rangle_c)^2 \\ &+ 6(\langle a_m\rangle_c - \langle a_m{}^2\rangle_c + \langle a_m{}^3\rangle_c/2)^2\cdot(\langle a_m{}^2\rangle_c - \langle a_m{}^3\rangle_c) \\ &+ (\langle a_m\rangle_c - \langle a_m{}^2\rangle_c + \langle a_m{}^3\rangle_c/2)^4\} \\ &+ \text{higher terms}\Bigg]\cdot\exp\{h(1)\}\,.\end{aligned} \tag{60}$$

[ ] represents the influence of the Bessel function of order zero. Equation (60) becomes Eq. (36) or (41) if [ ] is approximated by unit. The calculated results of $\langle a_m{}^n\rangle_c$ for the case of CO_2 and the influence of the Bessel function of order zero are given in Table 1.

TABLE 1. THE VALUES OF $\langle a_m{}^n\rangle_c$ AND THE INFLUENCE OF THE BESSEL FUNCTION IN REGARD TO CO_2
($\varepsilon\approx 1$. $\cosh 2\beta'\approx 1$. $P_e\approx P/B$. $P=70$ cmHg. $D=0.52$)

$\langle a_m{}^n\rangle_c$	$w=5$	$w=10$
$\langle a_m\rangle_c$	0.231	0.462
$\langle a_m{}^2\rangle_c$	0.054	0.232
$\langle a_m{}^3\rangle_c$	0.024	0.159
Influence of the Bessel function	1.020	1.035

$\langle a_m{}^n\rangle_c$ is given by

$$\langle a_m\rangle_c = (2\pi\varepsilon/D^2)\cdot\left(\frac{\langle k_{0m}\rangle_{av}+\langle k_{0m'}\rangle_{av}}{1+r}\right)\cdot P_e w$$

$$\langle a_m{}^2\rangle_c = (2\pi\varepsilon/D^2)^2\cdot\left(\frac{\langle k_{0m}^2\rangle_{av}+r\langle k_{0m'}^2\rangle_{av}}{1+r} - \frac{\langle k_{0m}\rangle_{av}^2+r\langle k_{0m'}\rangle_{av}^2}{1+r}\right)\cdot(P_e w)^2$$

---

[8] N. D. Coggeshall and E. L. Saiber, *J. Chem. Phys.*, **15**, 65 (1947).

$$\langle a_m{}^3\rangle_c=(2\pi\varepsilon/D^2)^3\cdot\left\{\frac{\langle k_{0m}^3\rangle_{av}+r\langle k_{0m'}^3\rangle_{av}}{1+r}\right.$$
$$-3\left(\frac{\langle k_{0m}^2\rangle_{av}+r\langle k_{0m'}^2\rangle_{av}}{1+r}\right)\cdot\left(\frac{\langle k_{0m}\rangle_{av}+r\langle k_{0m'}\rangle_{av}}{1+r}\right)$$
$$\left.+2\left(\frac{\langle k_{0m}\rangle_{av}^3+r\langle k_{0m'}\rangle_{av}^3}{1+r}\right)\right\}\cdot(P_e w)^3\,. \qquad (61)$$

0.52 is used for the value of D by means of Eqs. (40), (43) and the experimental data[1]

$$\frac{\langle k_{0m}^{1/2}\rangle_{av}+r\langle k_{0m'}^{1/2}\rangle_{av}}{(1+r)D}=8.0\times10^{-3}\,\mathrm{cm}^{-1/2}\cdot\mathrm{cmHg}^{-1}.$$

The influence of the Bessel function is thus proved to be within error. The experimental values are compared with the theoretical ones (Fig. 10). The dotted line shows the experimental curve and the solid line the theoretical curve given by

$$\ln\frac{1}{1-x}=8.60\times10^{-4}(P_e w)-8.00\times10^{-7}(P_e w)^2$$
$$+\,1.01\times10^{-9}(P_e w)^3. \qquad (62)$$

This is derived by substituting the values of (43) into Eq. (41) and using 0.52 for D. In order to attain a better agreement between theoretical and experimental values under high pressure, the value of 0.36 should be used as the correction factor D instead of 0.52. In case of CO,[9] similarly to CO_2, the value of 0.16 should be replaced with 0.07. These discrepancies seem to result from several assumptions, especially the roughness of the rectangular approximation concerning the shape of the absorption lines of the detector, and the conditions under which experiments correspond to the intermediate case of δ.

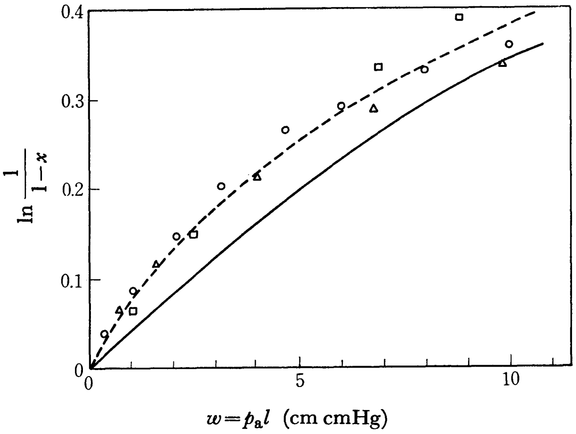

Fig. 10. The broken line; experimental. The solid line; theoretical.

---

[9] T. Yonezawa and E. Niki, *Trans. Soc. Instr. Cont. eng.*, **7**, 238 (1970).